

Thermal effects on the critical current of spin torque switching in spin valve nanopillars

M. L. Schneider,^{a)} M. R. Pufall, W. H. Rippard, and S. E. Russek
National Institute of Standards and Technology, Colorado 80305

J. A. Katine
Hitachi San Jose Research Center, San Jose, California 95120

(Received 6 September 2006; accepted 24 January 2007; published online 28 February 2007)

In spin valve nanopillars, temperature affects the spin torque reversal of the free magnetic layer. The authors compare values of zero temperature critical switching current I_{c0} extrapolated from room temperature pulsed current switching measurements to those of quasistatic current sweeps at 5 K. The values extrapolated from the room temperature pulsed switching probability measurements are always less than or equal to those of the low temperature quasistatic measurements. Further, the room temperature device-to-device variations of the critical switching current are drastically reduced at low temperature, where the I_{c0} agrees with theory. Finally, the authors find that I_{c0} scales with the free layer volume, as expected. © 2007 American Institute of Physics.

[DOI: 10.1063/1.2709963]

The spin torque effect is an efficient way to change the orientation of the free layer in a spin valve nanopillar with a high current density perpendicular to the film plane.¹⁻⁵ This effect has recently been demonstrated as a viable alternative to the cross-point writing scheme of conventional magnetic random access memory (MRAM).⁶ One of the reasons for pursuing alternative switching architecture is the scaling limitations of conventional MRAM. Spin torque switching of MRAM has the advantage that as the size of the devices is reduced, the current needed to switch the free layer orientation is decreased.^{1,7,8} However, one difficulty with implementing current perpendicular to plane (CPP) nanopillars in large scale commercial products is device-to-device variation of the magnetic properties, as well as the impact of these variations on the critical switching current I_c .⁸ We verified that these variations are dominated by thermal effects by comparing I_c at room temperature and 5 K for nine different devices. We also compare the values of I_c extrapolated from room temperature pulsed switching measurements to those determined from low temperature quasistatic switching measurements.

The samples used in this study were CPP giant magnetoresistance (GMR) spin valve nanopillars. The material was dc magnetron sputtered with the following structure: bottom lead Ta (0.5 nm) Cu (20 nm) Ta (3 nm) Cu (20 nm) Ta (2.5 nm)/antiferromagnet PtMn (17.5 nm)/synthetic antiferromagnetic pinned layer $\text{Co}_{80}\text{Fe}_{20}$ (1.5 nm) Ru (0.8 nm) $\text{Co}_{80}\text{Fe}_{20}$ (1.9 nm)/normal metal spacer layer Cu (4 nm)/free layer $\text{Co}_{80}\text{Fe}_{20}$ (1.0 nm) $\text{Ni}_{86}\text{Fe}_{14}$ (2.4 nm)/capping layer Cu (20 nm) Ru (50 nm) Ta (2.5 nm). Following deposition, electron-beam lithography was used to pattern the material into elongated hexagons with sizes of $50 \times 100 \text{ nm}^2$ and $75 \times 150 \text{ nm}^2$.⁸ The samples were fabricated without breaking vacuum in order to avoid sidewall oxidation which can further complicate device behavior at low temperature. We define positive bias current as electrons flowing from the free layer to the reference layer, and tends to align the two layers

in the antiparallel state. The reference layer is pinned along the easy axis (long axis of the hexagon). Positive applied field is defined along the easy axis in the direction of the magnetization of the pinned reference layer.

Previous studies have explored the inconsistencies of the critical current values for devices that have nearly the same resistance area product as those discussed here and have concluded that thermal effects at room temperature must be present in order to account for the variations.^{8,9} When the magnitude of the total field on the free layer (H_{free}) is less than the in-plane anisotropy of the free layer (H_k), one can use stability analysis^{9,10} on the Landau-Lifshitz-Gilbert equations of motion for the free layer in the device. When combined with the Slonczewski term⁷ for the spin-transfer torques, one can predict the critical instability current, which, in the case of precessional switching, is approximately the critical switching current in the absence of thermal effects, i.e., at $T=0$:⁸

$$I_{c0}^{\pm} = \left(-3.77 \times 10^9 \frac{1}{\text{A m}} \right) \frac{(\alpha M_s V)(H_k + H_{\text{free}} + (H_{\perp}/2))}{\nu^{\pm} P}, \quad (1)$$

where α is the Gilbert damping parameter, M_s is the saturation magnetization, V is the volume of the free layer of the spin valve, and H_{\perp} is the out-of-plane anisotropy. The polarization factor ν is defined as $\nu^{\pm}(\cos(\theta)) \equiv \pm 8\sqrt{P[(1+P)^3 + (3+\cos(\theta)) - 16P^{3/2}]^{-1}}$, where θ is the initial angle between the free and reference layers, P is the polarization, and \pm is when $\theta=0, 180^\circ$. Note that the coercivity H_c and H_{free} do not significantly contribute to the critical current at low temperature as they are much smaller than H_{\perp} . Neglecting H_c and H_{free} , I_{c0} depends only on the intrinsic magnetic parameters and not on the extrinsic parameters such as shape anisotropy or magnetostatic coupling between the layers, and so is a figure of merit by which one can compare different spin-transfer switching systems. We use values of $M_s = 800 \text{ kA/m}$, $\alpha = 0.02$, $H_{\perp} = 6.76 \times 10^5 \text{ A/m}$, $H_c = 6.4 \times 10^3 \text{ A/m}$, and $H_{\text{free}} = 0$. The values α and H_{\perp} are well known from other work;⁸ however, the polarization P is not

^{a)}Electronic mail: mlschnei@boulder.nist.gov

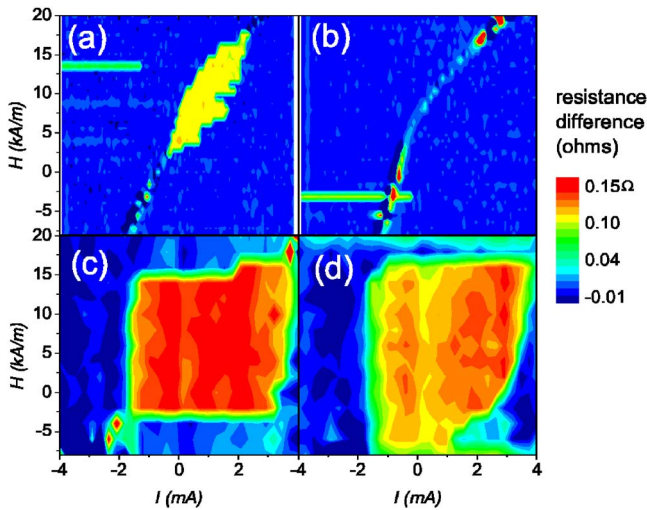


FIG. 1. (Color online) Differential resistance vs current and field for a $50 \times 100 \text{ nm}^2$ elongated hexagon sample. The negative going current sweep was subtracted from the positive going current sweep to find hysteretic regions of the device. (a, upper left) room temperature scan of device 1, (b, upper right) room temperature scan of device 2, (c, lower left) low temperature scan of device 1, and (d, lower right) low temperature scan of device 2.

well known. One would expect a value on the order of 0.3 for an all metallic device as derived in Ref. 7. However, the synthetic antiferromagnetic layer may result in a value that is less than that of a simple two magnetic layer metallic device.⁸

Low temperature quasistatic switching measurements were performed in a liquid helium flow cryostat with the sample in vacuum. The measurement probes were thermally anchored to the cold stage and reached an ultimate temperature of 18 K. The substrate was thermally connected to the cold stage and was held at 5 K. There was some additional heating from the dc bias current, which is discussed below.

Figure 1 shows the quasistatic current induced hysteresis of two $50 \times 100 \text{ nm}^2$ devices at room temperature and 5 K as a function of current and field; the left column is labeled as device 1 and the right column as device 2. Both devices have nominally $10.7 \pm 0.1 \Omega$ resistance. The plots in Fig. 1 are based on the differential resistance curves such as that in Fig. 2(a). In Fig. 1, the differential resistance curves for the two current sweep directions are subtracted, leaving only the hysteretic behavior. Note that all of the color scales and axes of the four graphs of Fig. 1 are identical. Figure 1(a) shows a device with a relatively large hysteretic region at room temperature, while device 2, Fig. 1(b), exhibits effectively no hysteresis. The horizontal lines in Figs. 1(a) and 1(b) are not part of the device response, but are artifacts from changes in the contact resistance due to probe motion. While there are some differences in the device responses at low temperature, the maximum critical currents are nearly the same in Figs. 1(c) and 1(d). For device 1, the currents are -1.5 and 3.7 mA, and for device 2, they are -1.5 and 3.5 mA. These numbers are the average values for the critical currents for the sections of the hysteresis that did not vary strongly with applied field.

In order to find agreement with our experimental results and Eq. (1) the polarization must be 15% instead of the expected 30%. Transmission electron microscope cross sections suggest that, due to a sloped sidewall profile, the free layer is larger than the lithographic area. However, while this

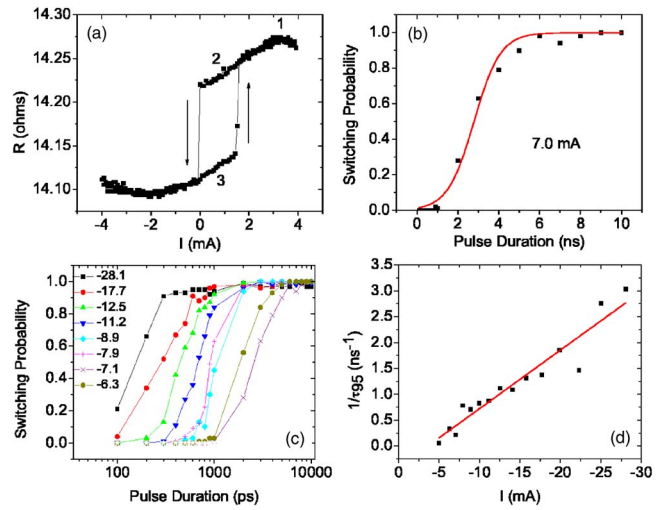


FIG. 2. (Color online) Data from a $75 \times 150 \text{ nm}^2$ elongated hexagon sample. (a, upper left) Typical room temperature differential resistance curve. The arrows indicate the directions along which the current was swept in the measurements. (b, upper right) Plot of switching probability vs pulse duration. The solid line is a fit by the Fermi function. (c, lower left) Switching probability vs pulse duration for several different current levels. (d, lower right) Value of τ_{95} , the pulse duration required for a 95% switching probability, vs the pulse current.

accounts for some of the polarization discrepancy, it does not account for the difference of a factor of 2 that we observe. Nonetheless, the use of 15% yields agreement for both the positive and negative critical currents, and scales correctly with device size, while simply increasing the value of α for example, does not. For a $50 \times 100 \text{ nm}^2$ elongated hexagon, Eq. (1) predicts $I_{c0}^- = -1.5$ mA and $I_{c0}^+ = 3.7$ mA. Our $T = 5$ K measurements of four devices of this size yielded average values of $I_{c0}^- = -1.5 \pm 0.3$ mA and $I_{c0}^+ = 3.7 \pm 0.1$ mA. To test the validity of these parameters, we performed the same measurement on $75 \times 150 \text{ nm}^2$ devices and found that Eq. (1) predicts $I_{c0}^- = -3.4$ mA and $I_{c0}^+ = 8.3$ mA, while our low temperature measurements of five devices of this size yield critical current values of $I_{c0}^- = -3.7 \pm 0.3$ mA and $I_{c0}^+ = 8.3 \pm 0.2$ mA, in good agreement with Eq. (1).

The variation in I_{c0} from device to device was drastically reduced at low temperature compared to room temperature quasistatic measurements of the switching current on the same devices. The agreement of I_{c0} between devices at low temperature was 40 times better than at room temperature. Furthermore, the values determined from the low temperature measurements were robust with respect to device size and in quantitative agreement with theoretical predictions from Eq. (1). Thus, we conclude that the room temperature device-to-device variations in the quasistatic switching behavior are dominated by thermal effects. At room temperature the non-negligible values of H_c and H_{free} in Eq. (1) may play some role in device-to-device variations for the quasistatic case.^{8,9}

While there are variations between devices that indicate nonsingle domain behavior, at low temperature the critical currents are largely the same for all devices with the same magnetic volume. One example can be seen by comparing Figs. 1(c) and 1(d). One would expect the edges of the hysteretic region at zero temperature to be straight lines. However, there is a rounding of the lower right corner suggesting nonsingle domain behavior of device 2. In addition, the overall hysteretic region of device 2 at low temperature is larger

than that of device 1 so one would expect it to have a larger hysteretic region at room temperature even including thermal effects,⁸ but this is not observed. In general, more than half of the devices exhibited nonsingle domain behavior such as rounding or variation in the field values that exhibit a hysteretic region. However, the low temperature critical currents were still quite consistent as can be seen in Fig. 1.

Because the critical currents measured at 5 K were consistent, we do not expect thermal variations from device to device to play an important role in our analysis. However, we know that there is Joule heating due to the bias current used during measurements. To make our estimate of the Joule heating, we measured the parabolic background in device resistance with respect to I_{c0} , and then measured the $I_c=0$ mA resistance at several temperatures and compared the two measurements. The heating varied by a small amount from device to device, and we found that repeated measurements of the same device showed more heating in the subsequent measurements indicating that the contacts were being worn over time, causing further heating at the contacts themselves rather than at the devices. However, we have no accurate way of determining the amount of heat that is transmitted from the contact to the devices so we use the value for the total heating as an upper limit. The heating of the samples at low temperature was typically on the order of 9 K/mA, which gives us a maximum heating of about 33 K for the -3.7 mA switching event. At room temperature the average heating was less than 2 K/mA for all devices. However, there are several other parameters in Eq. (1) that may vary with temperature and these may also account for some of the variations.

We have also compared the values of the critical currents determined above to those determined through room temperature pulsed switching measurements. The device response to high-speed current pulses was measured using a microwave probing assembly with a bandwidth of 18 GHz.⁴ Previous work has investigated pulse current switching characteristics at different current levels and pulse durations.^{1,4,5,11-13} In the higher current regime, where the switching time is less than 10 ns, the switching event is driven by precessional motion rather than thermal activation. Figure 2 shows the pulsed data analysis that was used to predict the low temperature switching current, as has been reported for current-in-plane spin valve devices¹⁴ as well as CPP spin valve devices.⁴ Figure 2(a) shows a typical plot of differential resistance versus dc current. In this pulsed measurement, a dc current of +3 mA was applied through the device for 1 s to set the device to the antiparallel state, corresponding to position 1 of Fig. 2(a). The dc current was then lowered to bias the device at the middle of its hysteretic region and its resistance measured to verify the free layer orientation [position 2 of Fig. 2(a)]. After the resistance measurement, the ac current was shut off and a negative current pulse was applied in an attempt to switch the free layer of the spin valve. If the switch occurs, the device would then be in position 3 of Fig. 2(a). After the current pulse, the final resistance state of the device was measured to determine if the device switched. This process was repeated 100 times to determine the switching probability for various pulse current amplitudes and durations for several devices.

Figure 2(b) shows a plot of switching probability versus pulse duration for a pulse amplitude of -7.0 mA. The solid red line fit is that of the Fermi function, which is used to

determine τ_{95} , the pulse duration necessary for a 95% switching duration.⁴ Figure 2(c) shows the results of switching probability versus pulse duration for several different current values. Each of these was fitted as shown in Fig. 2(b). The inverse of the pulse duration ($1/\tau$) for 95% switching probability is plotted versus current in Fig. 2(d). By linearly extrapolating the data to the switching time $\tau \rightarrow \infty$, we find a zero temperature switching current of $I_{c0} = -3.6$ mA.

These pulsed measurements were repeated on seven devices. The pulsed measurements yield agreement with the low temperature measurements only for some devices, with the lowest extrapolated critical current values being roughly half of the values determined through the low temperature quasistatic measurements. The agreement between the two methods to determine the critical current values is *not* improved by only fitting the highest current values, i.e., well into the precessional switching regime, in the pulsed measurements for all of the devices. We find that in all cases the absolute value of the critical current from the pulsed measurements was equal to or less than that measured at low temperatures. This may indicate that even the precessional switching regime events can be thermally assisted or that the devices are exhibiting nonsingle domain behavior. It should also be noted that the GMR and thus the polarization, as well as M_s , α , and the various anisotropies, are somewhat temperature dependent. Without the presence of an oxide, M_s , α and H_{\perp} should vary by 10% or less, while the GMR varies by about a factor of 1.5. These variations would most likely have a small but canceling effect between room temperature and 5 K measurements.

In conclusion, the variations in the hysteretic region of the free layer at room temperature are dominated by thermal effects. Further, we find that these device-to-device variations can affect the room temperature pulsed switching probabilities and the value of the zero temperature critical current extrapolated from them. With the thermal effects reduced, the theory of Slonczewski accurately predicts the critical current necessary to switch the orientation of the free layer of CPP nanopillars.

¹F. J. Albert, N. C. Emley, E. B. Myers, D. C. Ralph, and R. A. Buhrman, Phys. Rev. Lett. **89**, 226802 (2002).

²F. J. Albert, J. A. Katine, R. A. Buhrman, and D. C. Ralph, Appl. Phys. Lett. **77**, 3809 (2000).

³S. Urazhdin, N. O. Birge, W. P. Pratt, and J. Bass, Phys. Rev. Lett. **91**, 146803 (2003).

⁴S. Kaka, M. R. Pufall, W. H. Rippard, T. J. Silva, S. E. Russek, J. A. Katine, and M. Carey, J. Magn. Magn. Mater. **286**, 375 (2005).

⁵R. H. Koch, J. A. Katine, and J. Z. Sun, Phys. Rev. Lett. **92**, 088302 (2004).

⁶M. Hosomi, H. Yamagishi, T. Yamamoto, K. Bessho, Y. Higo, K. Yamane, H. Yamada, M. Shoji, H. Hachino, C. Fukumoto, H. Nagao, and H. Kano, Tech. Dig. - Int. Electron Devices Meet. **2005**, 459.

⁷J. C. Slonczewski, J. Magn. Magn. Mater. **159**, L1 (1996).

⁸D. Lacour, J. A. Katine, N. Smith, M. J. Carey, and J. R. Childress, Appl. Phys. Lett. **85**, 4681 (2004).

⁹N. Smith, e-print cond-mat/0406486.

¹⁰J. Grollier, V. Cros, H. Jaffres, A. Hamzic, J. M. George, G. Faini, J. Ben Youssef, H. Le Gall, and A. Fert, Phys. Rev. B **67**, 174402 (2003).

¹¹E. B. Myers, F. J. Albert, J. C. Sankey, E. Bonet, R. A. Buhrman, and D. C. Ralph, Phys. Rev. Lett. **89**, 196801 (2002).

¹²K. Yagami, A. A. Tulapurkar, A. Fukushima, and Y. Suzuki, IEEE Trans. Magn. **41**, 2615 (2005).

¹³N. C. Emley, I. N. Krivorotov, O. Ozatay, A. G. F. Garcia, J. C. Sankey, D. C. Ralph, and R. A. Buhrman, Phys. Rev. Lett. **96**, 247204 (2006).

¹⁴S. Russek, R. D. McMichael, M. Donahue, and S. Kaka, in *SpinDynamics*, edited by B. Hillebrands (Academic, New York, 2003), Vol. II, pp. 93-154.